Am. J. Hum. Genet. 65:318–326, 1999

The Molecular Basis of Malonyl-CoA Decarboxylase Deficiency

David R. FitzPatrick,[1] Alison Hill,[1] John L. Tolmie,[3] David R. Thorburn,[2] and John Christodoulou[4]

[1]Human and Clinical Genetics Units, Molecular Medicine Centre, Western General Hospital, Edinburgh; [2]The Murdoch Institute, Royal Children's Hospital, Melbourne, Australia; [3]Duncan Guthrie Institute, Yorkhill, Glasgow; and [4]Western Sydney Genetics Program, Royal Alexandra Hospital for Children and Department of Paediatrics and Child Health, University of Sydney, Sydney, Australia

Summary

We characterized a 2.1-kb human cDNA with a 1362-bp (454–amino acid) open reading frame showing 70.3% amino acid identity to goose malonyl-CoA decarboxylase (MCD). We have identified two different homozygous mutations in human MCD (hMCD) by using RT-PCR analysis of fibroblast RNA from two previously reported consanguineous Scottish patients with MCD deficiency. The first mutation is a 442C→G transversion resulting in a premature stop codon (S148X) in the N-terminal half of the protein. The second is a 13-bp insertion in the mature RNA, causing a frameshift with predicted protein truncation. This insertion is the result of an intronic mutation generating a novel splice acceptor sequence (IVS4–14A→G). Both mutations were found to segregate appropriately within the families and were not found in 100 normal unrelated individuals. These mutations would be predicted to cause MCD deficiency, thus confirming this transcript as the hMCD ortholog. The peptide sequence of hMCD revealed a C-terminal peroxisomal targeting sequence (-SKL). This targeting signal appears to be functional in vivo, since the distribution of MCD enzymatic activity in rat liver homogenates—as measured by means of subcellular fractionation—strongly suggests that MCD is localized to peroxisomes in addition to the mitochondrial localization reported elsewhere. These data strongly support this cDNA as encoding human MCD, an important regulator of fatty acid metabolism.

Introduction

Malonyl-CoA decarboxylase (MCD; EC 4.1.1.9) catalyzes the conversion of malonyl-CoA to acetyl-CoA. MCD activity has been detected in both prokaryotes and eukaryotes, but its only proven in vivo role is in the production of erythromycin in bacteria (Hsieh and Kolattukudy 1994). The cellular function of mammalian MCD is not known. It may play a role in the regulation of fatty acid synthesis and oxidation via the potent inhibitor of mammalian carnitine palmitoyltransferase I (CPT1) by malonyl-CoA (Shi et al. 1998). The best evidence for a critical role for MCD in any vertebrate species comes from the study of a rare inborn error of metabolism in humans. To date, seven cases of human MCD deficiency (MIM 248360) have been reported (table 1). This condition is present in early childhood and is associated with malonic aciduria (7/7), methylmalonic aciduria (7/7), developmental delay (7/7), seizure disorder (4/7), hypoglycemia (4/7), and cardiomyopathy (2/7). In this study, we report the characterization of a human MCD (hMDA) cDNA and the identification of causative mutations in the hMCD gene in two patient samples, and we present evidence that MCD is localized to both mitochondria and peroxisomes in mammalian cells.

Material and Methods

Identification of hMCD cDNA and Genomic Clones

The TBLASTN program was used to search dbEST by means of the goose MCD peptide (gMCDp) sequence (dbEST database; GenBank P12617). The sequences identified were extended, and a consensus sequence was generated by means of the ESTblast program (ESTblast). Clones, obtained from the IMAGE consortium HGMP, were then sequenced in both directions to confirm the previous sequence and to fill in gaps. The sequence-tagged site (STS) WI-11775, derived from one of the cDNAs identified by TBLASTN searching, was used to identify two human genomic clones from the de Jong RPCI1 gridded P1 artificial chromosome (PAC) library by means of PCR pools (supplied by the HGMP resource center). Both cDNA and genomic sequencing were performed by use of the ThermoSequenase cycle sequencing kit with ^{33}P-labeled dideoxynucleotides (Amersham). Northern blot analysis was performed by use of Multiple

Received October 26, 1998; accepted for publication May 20, 1999; electronically published July 13, 1999.

Address for correspondence and reprints: Dr. David R. FitzPatrick, Human and Clinical Genetics Units, Molecular Medicine Centre, WGH, Edinburgh EH4 2XU, UK. E-mail: david.fitzpatrick@ed.ac.uk

0002-9297/99/6502-0007/02.00

Table 1

Clinical Features of Patients with MCD Deficiency

Author(s) (year)	Consanguinity	Age	Delayed Neurological Development	Seizures	Short Stature	Sib Death	Acidosis	Hypoglycemia	Cardiomyopathy
Brown et al. (1984)	Yes	5 years	Yes	No	Yes	Yes	Yes	No	No
Haan et al. (1986)	No	10 mo	Yes	No	No	No	Yes	Yes	No
Matalon et al. (1993)	No	7 mo	Yes	Yes	No	No	No	No	Yes
MacPhee et al. (1993)	Yes	3.9 years	Yes	Yes	No	No	No	No	No
MacPhee et al. (1993)	Yes	13 years	Yes	Yes	No	No	No	Yes	No
Krawinkel et al. (1994)	Yes	4 d	Yes	No	No	Yes	Yes	Yes	No
Yano et al. (1997)	No	4 years	Yes	Yes	No	No	Yes	Yes	Yes

NOTE.—All patients were alive at the time of publication in July 1999.

Choice Northern Blot (OriGene), according to manufacturer's instructions.

Fibroblast Culture, RT-PCR Analysis, and Characterization of Mutations

Fibroblast cells from two children with MCD deficiency (designated "case 1" and "case 2," as in the original report; MacPhee et al. 1993) and four unrelated control fibroblast lines were cultured in Eagle's Basal Medium with 10% fetal calf serum, 100 U/ml penicillin, and 100 μg/ml streptomycin. The fibroblasts were harvested by means of a solution containing trypsin 0.025 g/100 ml, 0.5 mM EDTA (trypsin/EDTA). Total cellular RNA was prepared by means of the RNA Isolation kit (Stratagene). Five micrograms of total cellular RNA from each fibroblast line were reverse transcribed by means of the RT-PCR kit (Stratagene), according to the manufacturer's instructions. PCR amplification of the coding region was done in seven different reactions by using primer pairs MCD1-7 (table 3) under standard reaction conditions (Saiki et al. 1988). PCR cycle conditions were identical for all primer pairs by using a hot-start (80°C × 3 min, 94°C × 2 min) followed by a touch-down PCR with common denaturation and extension segments (94°C × 30 s, 72°C × 1 min) and the following annealing segments (59°C × 30 s, 2 cycles; 58°C × 30 s, 2 cycles; 57°C × 30 s, 30 cycles), followed by a final extension segment (72°C × 5 min). SSCP was done by means of standard techniques (Axton et al. 1997). Direct sequencing of RT-PCR products was achieved by using a ThermoSequenase cycle sequencing kit with ^{33}P-labeled dideoxynucleotides (Amersham). Mutagenically separated PCR (MS-PCR) assays (Rust et al. 1993) for the 442C→G and IVS4 -14A→G mutations used primer sets MCD8 and MCD9, respectively (table 3).

Rat Liver Subcellular Organelle Isolation

Adult male Sprague-Dawley albino rats (150–210 g) were killed by carbon dioxide asphyxiation, after which their cervices were dislocated and their livers excised. The protocol used for isolation of subcellular organelles is essentially as described elsewhere (Singh and Poulos 1988), except that the pooled 16,500 g supernatants and the crude peroxisomal fractions were centrifuged at 100,000 g for 60 min.

Enzyme Assays

MCD (E.C. 4.1.1.9) was assayed radiochemically. The reaction mixture (volume 400 μl) contained 50 mM KPi (pH 7.4), 253 μM [1,3 ^{14}C]malonyl-CoA (New England Nuclear Research Products, specific activity 0.75 mCi/mmol), cell extract, and BSA to give a total protein concentration in the reaction mixture of $\geq$0.4 mg/ml. The reaction mixture was incubated for 3 h at 37°C and the evolved $^{14}CO_2$ was trapped and counted (Fox 1971). For

Table 2

ESTs Identified with Significant Homology to gMCDp Sequence

EST Name	Clone ID	Length (bp)	Source Library	End	Homology[a]	Blast Score
AI123407	1690076	641	Mixed	5′	53–253	275
AA291121	700476	329	Germinal Centre B cell	5′	347–455	324
AA333449	135110	247	8-wk embryo	5′	183–263	277
AA340389	142028	224	Fetal brain	5′	429–502	300
R08989[b]	127540	371	Fetal liver and spleen	5′	395–442	166

[a] Region of amino acid homology to the gMCD sequence (GenBank P12617).

[b] Sequence from the 3′ end of this clone was previously used to design the hMCD STS WI-11775.

Table 3

Intron-Exon Boundaries of hMCD

No.	5′ Junction	Exon Size	3′ Junction
1		410[a]	ATCCAGgtaagggg
2	cttttcagGAAATG	113	CAGTGAgtaagtat
3	gcccccagGGCTGA	156	ATCCAGgtacctgc
4	ttttccagGCAATC	150	TTGCAGgtaagcga
5	ctttacagAGAGAG	~1230	

[a] Number of bases from start of initiating codon to 3′ junction of first exon.

the pH optima studies, a buffer solution consisting of 50 mM Mes, 25 mM Tris, 25 mM ethanolamine, and 100 mM sodium chloride with the pH for each buffer adjusted to 4.5–10 with either hydrochloric acid or sodium hydroxide was used instead of the potassium phosphate buffer. Citrate synthase (CS; mitochondrial marker enzyme), catalase (peroxisomal marker enzyme), and NADPH-cytochrome c reductase (NADPHCR; microsomal marker enzyme) were all assayed as described elsewhere (Sottocasa et al. 1967; Shepard and Garland 1969; Aeib 1974). Lactate dehydrogenase (LDH; cytoplasmic marker enzyme) was assayed by means of a modification of a previously published method (Bergmeyer and Bernt 1974). The reaction mixture (total volume 1 ml) consisted of 50 mM potassium phosphate buffer, pH 7.4, 1 mM pyruvate (freshly made each day), 0.25 mM NADH, and the cell fraction (5–70 mg protein). The rate of oxidation of NADH was followed spectrophotometrically at 340 nm. All assays were performed in duplicate, and the results shown are means. Protein levels were measured spectrophotometrically (Lowry et al. 1951) or fluorometrically (Udenfriend et al. 1972), with BSA as the standard.

Results

hMCD cDNA

A TBLASTN search (Altschul et al. 1990) with the gMCDp sequence identified five highly homologous human-expressed sequence tags (ESTs) (table 2), and subsequent BLASTN and estBLAST searches identified an additional nine cDNA clones. Six of these clones were obtained and sequenced, and a 2117-base consensus sequence encoding a 1,362-base (454–amino acid) open reading frame (ORF) was submitted to GenBank (AF097832). Screening of 5×10^5 primary clones from a human fetal muscle cDNA library (HGMP) identified three additional clones, all truncated at the 5′ end. 5′ rapid amplification of cDNA ends (RACE) analysis by use of polyA+–selected RNA from fibroblasts and total RNA from human fetal muscle failed to identify new sequence information.

The position of the proposed initiating methionine codon in the hMCD cDNA is identical to that of a translation start site identified in the goose (Courchesne Smith et al. 1992). The sequence surrounding this AUG codon was analyzed by means of the human data available from the TransTerm database. This analysuis demonstrated a good consensus initiation sequence context on the basis of >6,000 sequences in the public databases. The observed likelihood of each base being observed at a set position from the initiation codon was compared to the sequence of MCD. The bases 5′ of the AUG (GGGCC) were seen in 29%, 25%, 38%, 40%, and 48%, respectively, of known initiation sequences. The equivalent figures for the bases 3′ of the AUG (GACGA) were 49%, 27%, 27%, 37%, and 26%. Although the ORF in the human transcript continued 5′ of this AUG for ⩾60 bases, no other in-frame AUG or stop codons could be identified. However, no significant amino acid homology with the "extra" 50 amino acids of the goose peptide could be detected in any reading frame in the human ORF 5′ to the ATG.

Genomic Clone Analysis

Two human genomic PAC clones were isolated by use of an STS WI-11775, described elsewhere (Schuler et al. 1996), which was used to map one of the MCD EST clones on radiation hybrid panels. Direct sequencing of these PAC clones revealed five exons (table 3) with perfect conservation of the position of the intron-exon boundaries between the human and goose genes (Courchesne Smith et al. 1992). Unfortunately, sequencing of the 5′ end of this gene has proven very difficult because of the high CG content. We are currently making a small insert library from these PAC clones to facilitate identification of other possible 5′ coding regions and promoter sequences.

Tissue Distribution of hMCD

We were unable to identify a hybridization signal by using a 1.8-kb hMCD cDNA probe on a commercial northern blot made with 2 μg polyA+–selected RNA from several human tissues including heart, liver, and brain (data not shown). This problem was expected from work done elsewhere (Jang et al. 1989) on the goose, in which very large amounts of polyA+ RNA (>100 μg) were required to detect any MCD hybridization signal on a northern blot. PCR analysis of human cDNA obtained from HGMP yielded a faint product in fetal muscle cDNA but no visible product in either placental or HepG2 cDNA. Interestingly, RT-PCR reactions using normal human fibroblast RNA yielded product with every primer pair tested.

Predicted hMCD Protein Product

The hMCD cDNA has an ORF of 454–amino acid product that shows 70.3% amino acid identity to g-

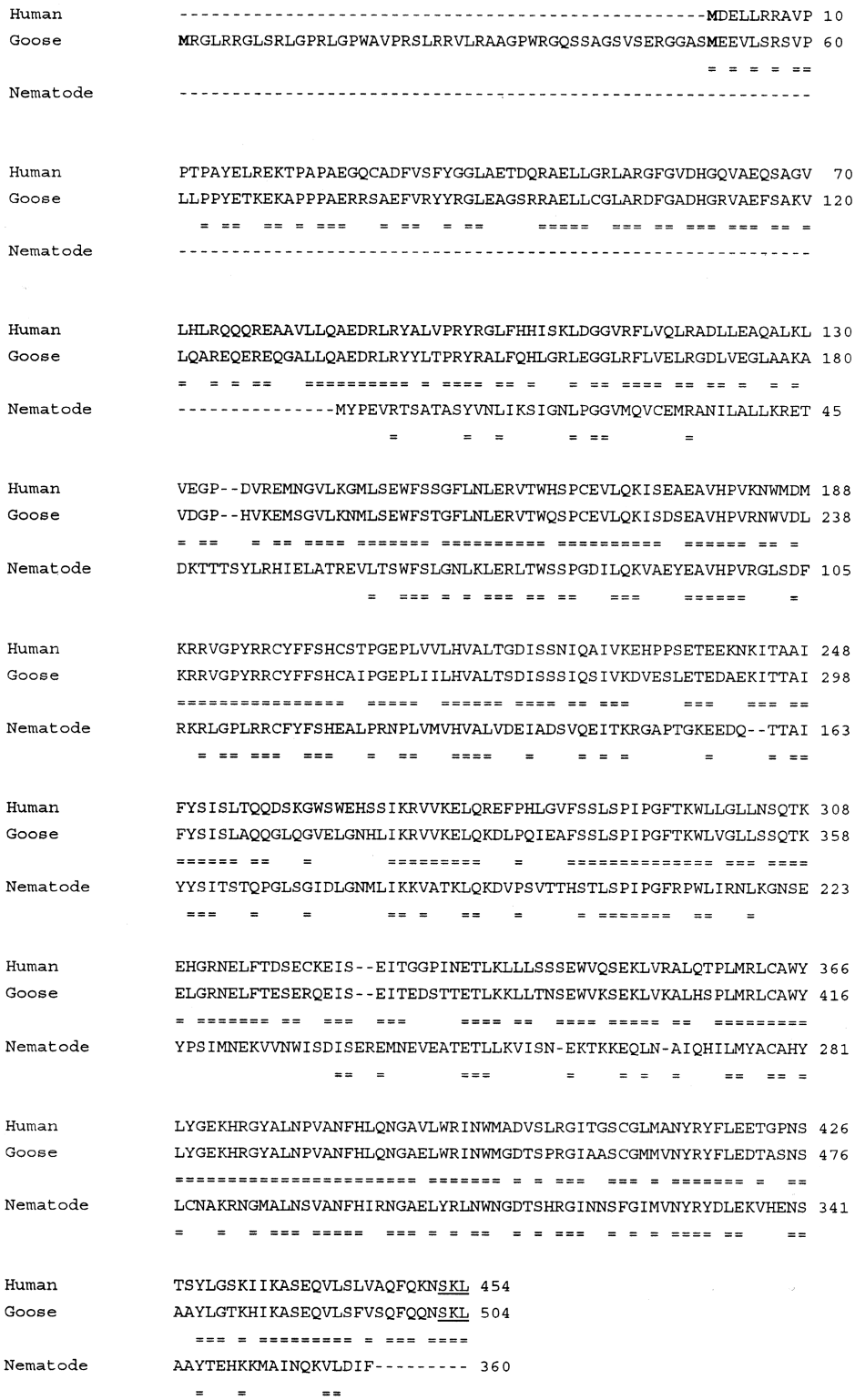

Figure 1 Alignment of the predicted hMCDp (GenBank AF097832) and gMCDp (GenBank P12617) sequences by use of ClustalW interactive analysis program (ClustalW). This shows 70.3% identity of >454 amino acids. The two characterized initiating methionines of the goose peptide are shown in boldface type (position 1 and 50). C-terminal peroxisomal-targeting sequences were identified in both human and goose sequences (-SKL) and are underlined. An ORF predicting a 360–amino acid peptide (GenBank Z46242) from a *C. elegans* gene (labeled "Nematode") from chromosome III also showed a high degree of homology on searching and is likely to be orthologous. There was 35.8% sequence identity among all three peptides.

MCDp on ungapped alignment (fig. 1). A predicted gene on *C. elegans* chromosome III (GenBank Z46242) encodes the only other highly homologous peptide (35.8% amino acid identity) identified by public database searches. A potential peroxisomal (-SKL) targeting sequence (Gould et al. 1990) was present at the C-terminus of the human protein. No other specific protein domains were recognized, and, in particular, no mitochondrial targeting sequence (MTS) could be identified.

Mutations in hMCD

RT-PCR analysis was performed on fibroblast RNA from two Scottish patients with MCD deficiency (cases 1 and 2), reported elsewhere (MacPhee et al. 1993), and four control cell lines. The coding region was amplified with primer pairs MCD1-7, listed in table 4. The RT-PCR products were then analyzed by SSCP and direct sequencing. Probable causative homozygous mutations were identified in both patients. The patient in case 1 was found to have an SSCP band shift by means of primer pairs MCD3 and MCD4 (fig. 2*A*). Direct sequencing of these PCR products revealed an apparently homozygous 13-bp insertion, rather than the wild-type sequence. This insertion was apparent on agarose gel electrophoresis with no evidence of the wild-type sequence in either this analysis or the silver-stained SSCP gel (fig. 2*A*). To clarify the genomic basis of this mutation, the genomic PAC clone was directly sequenced by use of the primer MCD4R. This revealed an intron-exon junction in the position predicted from the known goose sequence (table 3). It was noted that the sequence 5′ of the splice acceptor site in normal DNA was identical to the 13 bases inserted into the mRNA of the patient in case 1. Primer pair MCD10 was designed to amplify this region from genomic DNA. Direct sequencing of this product by means of genomic DNA from the patient in case 1 revealed an apparently homozygous A→G substitution at position −14 in intron 4 (fig. 2*B*). This mutation (IVS4 –14A→G) showed appropriate segregation within the family (fig. 2C) and was not detected in anonymous testing of 100 normal unrelated individuals from the cystic fibrosis screening program by means of an MS-PCR assay.

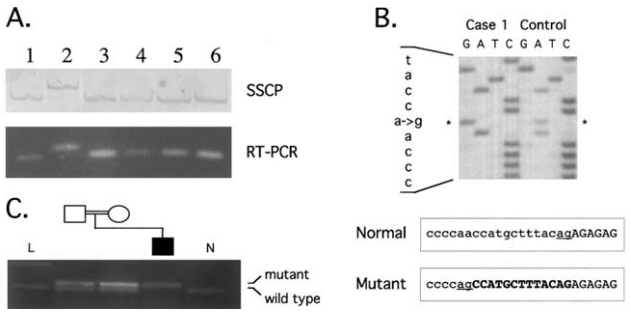

Figure 2 Case 1 mutation. *A*, Electrophoresis of RT-PCR products from the patients in case 2 (*lane 1*) and in case 1 (*lane 2*) and from the controls (*lanes 3–6*), with use of primer pair MCD3 with silver-stained SSCP (*top*) and primers MCD4F and MCD3R (predicted normal product size of 105 bp) with ethidium bromide–stained agarose gel analysis (*bottom*). Both analyses show a larger fragment in case 1, with no evidence of a normal band. *B*, Sequence of genomic PCR product from the patient in case 1 and a normal control showing A→G at position −14 in intron 4 (IVS4 –14A→G). The larger fragment shown in *A* was due to the creation of a novel 3′ splice site within the intron, thus creating the 13-bp insertion in the cDNA (CCATGCTTTACAG), as detailed in the two bottom panels. *C*, 2% agarose gel electrophoresis of MSPCR products by means of primer-set MCD8, showing appropriate segregation of the mutation within the nuclear family of the patient in case 1 (*lane 4*), homozygous mutant larger band (113 bp) for patients with both parents heterozygous (*lanes 2 and 3*), and a normal control homozygous smaller band (93 bp, *lane 5*). The DNA size marker ladder (L) shows 100-bp (*lower*) and 200-bp (*upper*) bands in lane 1.

Table 4

Primers Used for PCR Amplification

Name[a]	Forward	Reverse	Product Size
MCD1	AGGCGAGGACCGGCTGCG	GCCAGGTAACCCGTTCTAGGTTCAG	231
MCD2	AATGAATGGGGTGCTGAAAG	ATGGAGGATGTTCCTTCACG	293
MCD3	GTGGCACTGACTGGTGACAT	ACCCCAAGGTGAGGAAACTC	209
MCD4	ATTCCATCAGCTTGACCCAG	GGAGCTTGAGGGTCTCGTTA	267
MCD5	TCGTCAAGGAGTTGCAGAGA	CTCCATACAGGTACCAGGCG	294
MCD6	CCCATTAACGAGACCCTCAA	CTCCTCCAGGAAGTAGCGGT	273
MCD7	CCAACTTCCACCTGCAGAAC	GATCGTTTTCTTAGCCGGG	270
MCD8 (MT)	GGTGCTCCTCTGTTGGTAACGTA	AGACTTGAAAACACCCCAAGGTGAGGAAACTCT CTCTGTAAAGCATCGC	113
MCD8 (WT)	GGTGCTCCTCTGTTGGTAACGTA	GTGAGGAAACTCTCTCTGTAAAGCATGCT	93
MCD9 (MT)	TATCTTCTCCTTTTCAGGAAATGAATGGGG TGCTGAAAGGAATGCTCGG	ACTTACTCACTGATTTTCTGAAGCAC	138
MCD9 (WT)	ATGAATGGGGTGCTGAAAGGAATGCGCTC	ACTTACTCACTGATTTTCTGAAGCAC	118
MCD10	GACCGCTACACAGCAGCAT	TTCCGAATCTGTAAAGAGTTCA	244

[a] MT = mutant allele; WT = normal (wild-type) allele.

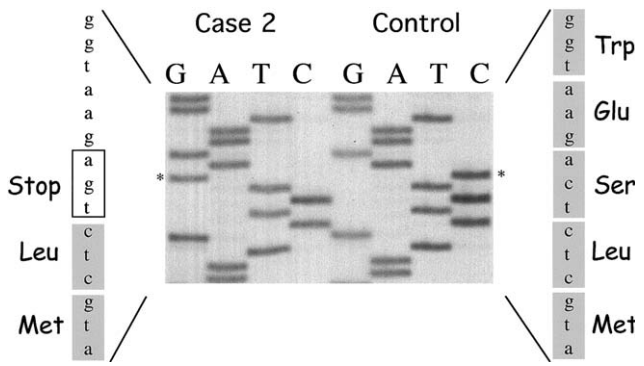

Figure 3 Case 2 mutation. Sequences of RT-PCR product from patient in case 2 and a healthy control show an apparently homozygous C→G transversion at nucleotide 442 in the cDNA, denoted by an asterisk (*). This results in the change of a serine codon (TCA) to a stop codon (TGA) at position 148 in the peptide (S148X).

In the patient in case 2, direct sequencing of the PCR yielded by primer pair MCD1 showed a C→G substitution at nucleotide 442 in the apparently full-length cDNA. This results in the formation of a premature stop codon (S148X) in the N-terminal half of the wild-type peptide (fig. 3). An MS-PCR assay was developed for this mutation, which confirmed the parents as heterozygous. This mutation was not detected in anonymous testing of 100 normal unrelated individuals from the cystic fibrosis screening program.

Subcellular Localization of MCD in Rat Liver

The results of enzyme assays of the organelle fractions obtained from rat liver are shown in figure 4. There was enrichment of catalase in the peroxisomal fraction and CS in the mitochondrial fraction, whereas NADPHCR was highest in the microsomal fraction. LDH activity was highest in the final supernatant. In addition, it can be seen that there was little contamination of mitochondria in the peroxisomal fraction (low CS activity) and little contamination of peroxisomes in the mitochondrial fraction (low catalase activity). There was, however, some microsomal contamination of peroxisomes (high levels of NADPHCR). It is of note that comparable MCD activity was found in both the mitochondrial and the peroxisomal fractions, clearly indicating that peroxisomes have MCD activity of their own far outweighing any potential contamination by mitochondrial MCD. This set of experiments was repeated twice with the same overall marker enzyme pattern being found, although the absolute specific activities differed somewhat.

MCD activity in mitochondrial and peroxisomal fractions was assayed in duplicate at 0.5 unit intervals from pH 4.5–10.0. The mean values of the specific activities are plotted in figure 5. It can be seen that the pH optima for the two forms of the enzyme are quite similar. Maximal activity for both the mitochondrial and peroxisomal enzymes was found at pH 5.0, with a secondary peak at pH 8.0–8.5 (peroxisomal form).

Discussion

The evidence that the cDNA presented in this report encodes hMCD has three main components. First, there is very highly significant sequence homology between the putative hMCD and the goose MCD (gMCD) at the level of both cDNA and predicted peptides. When compared to the goose gene, there is also perfect conservation in the position of the human intron-exon junctions. Second, we report that different homozygous mutations have been identified in two patients previously found to be deficient in MCD enzyme activity. Both these mutations are predicted to result in premature truncation in the N-terminal half of the protein, and it is highly likely that these represent loss-of-function mutations. Third,

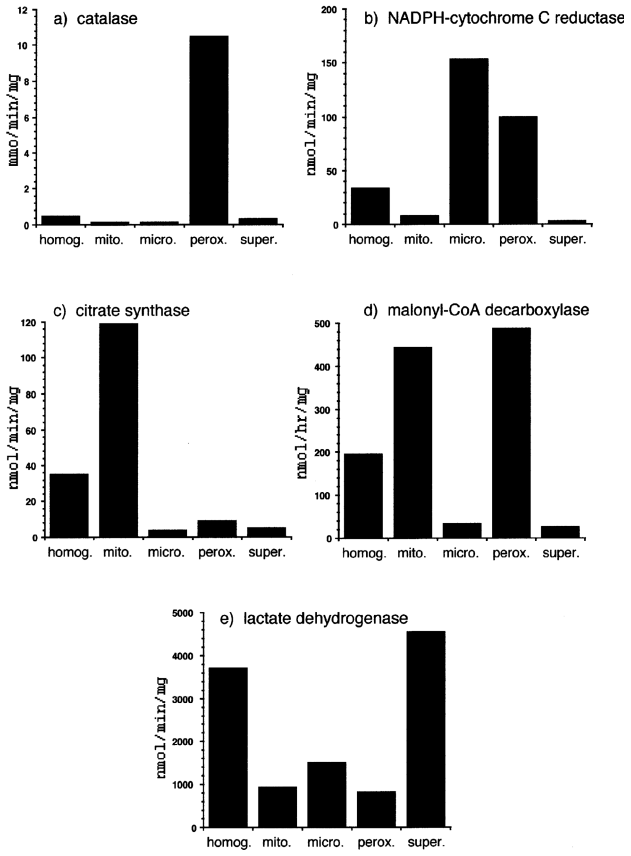

Figure 4 Marker-enzyme studies of rat liver organelle fractions. Enzyme activities were assayed in duplicate. The means of the specific activities are plotted for each organellar fraction. Abbreviations: homog. = homogenate; mito. = mitochondrial fraction; micro. = microsomal fraction; perox. = peroxisomal fraction; and super. = supernatant.

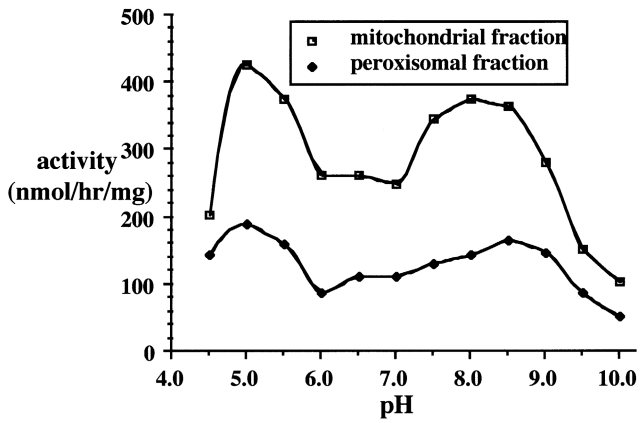

Figure 5 pH studies of rat liver mitochondrial and peroxisomal preparations. MCD activity was assayed in duplicate. The means of the specific activities are plotted for each organellar fraction. Two peaks—one at pH ~4.5–5.0 and the second at pH ~8.0–8.5—could be identified for both preparations.

the discovery of a C-terminal peroxisomal targeting sequence in hMCD peptide (hMCDp) correctly predicted the dual localization of MCD enzyme activity in mammalian cells. Peroxisomal localization of MCD has not been reported elsewhere.

The subcellular localization of MCD has been most extensively studied in the uropygeal (preening) gland of the domestic goose. In this tissue, it is expressed at a remarkably high level, accounting for ~1% of cellular protein (Kim and Kolattukudy 1978*b*). MCD activity is probably required to promote methylmalonyl-CoA (via methylmalonyl-acyl carrier protein) as a substrate for fatty acid synthase, thus enabling the synthesis of multiple methyl-branched fatty acids (Kolattukudy et al. 1987). Characterization of the goose cDNA and genomic structure revealed an interesting mechanism for the control of subcellular localization of MCD (Jang et al. 1989; Courchesne Smith et al. 1992). This gene uses two alternative transcription start sites that result in tissue-specific control of subcellular localization of the protein product. The larger transcript is translated to a 55-kDa protein with an N-terminal MTS; the smaller transcript produces a protein that is 5 kDa smaller than the mitochondrial form and was thought to result in a cytosolic protein. The position of the initiating methionine codon in this smaller transcript in the goose is identical to the putative initiating codon in the human cDNA (fig. 1). This would strongly argue that the human cDNA encodes a functional MCD protein. It is interesting to note that the studies on subcellular localization of the goose protein did not use peroxisomal markers (Scholte 1969; Kim and Kolattukudy 1978*a*). It may be useful to reassess these studies in view of the fact that the gMCDp also has a predicted C-terminal peroxisomal targeting sequence (-SKL) (Gould et al. 1990).

In humans, the best information regarding the subcellular localization of MCD comes from the study of urinary metabolites in human patients deficient in this enzyme activity. The presence of methylmalonic aciduria in MCD deficiency is thought to be because of the inhibition of the mitochondrial enzyme methylmalonyl-CoA mutase by malonyl-CoA. Intramitochondrial formation of malonyl-CoA is thought to occur as a result of low-level carboxylation of acetyl-CoA by propionyl-CoA carboxylase. Malonyl-CoA cannot be transported into or out of the mitochondrion; thus, MCD has a scavenging function in this organelle. It was expected that cloning of the 5′ end of the hMCD gene would identify an MTS in hMCDp. This prediction was made on the basis of the functional MTS identified in the gMCDp sequence (Courchesne Smith et al. 1992) and previous subcellular localization studies of mammals (Scholte 1969; Kim and Kolattukudy 1978*a*). However, in spite of extensive dbEST searching, cDNA-library screening, 5′ RACE, and genomic sequencing, an MTS could not be identified by use of the MitoProt II program (Claros and Vincens 1996).

The failure to identify an MTS may simply reflect the fact that we have not identified the full-length MCD transcript. Since we have been unable to size either the mRNA or native peptide, it is not possible to exclude the presence of another 5′ exon that encodes the "missing" mitochondrial targeting information. Sequencing the PAC clones containing the MCD gene and the production of MCD antisera will help clarify the situation. It is also possible that an MTS exists in our sequence but cannot be identified by current computer prediction programs. In any event, since the sequences flanking the putative AUG have a good Kozak consensus sequence and since an equivalent initiation codon is used in the goose, it is reasonable to assume that it may also be used to initiate translation in humans and produce a functional protein.

The localization of MCD to both mitochondria and peroxisomes may be important in the regulation of fatty acid oxidation via the powerful inhibition of CPT1 by malonyl-CoA (A'Bhaird and Ramsay 1992). Acetyl-CoA carboxylase (ACC), a cytoskeleton-associated enzyme (Geelen et al. 1997), is the only enzyme proven to synthesize malonyl-CoA. The role of ACC in malonyl-CoA-mediated regulation of fatty acid oxidation has been well studied (Zhang and Kim 1996; Abdel-Aleem et al. 1998). In contrast, little is known of the role that MCD plays in this system. It will be particularly important to investigate the possible role of MCD in cardiomyocytes (Hall et al. 1996; Dyck et al. 1998), given the finding of cardiomyopathy in some patients with MCD deficiency. The two reported patients with cardiac involve-

ment had chronic malonic aciduria, in contrast to the other patients, whose urine malonate tended to be elevated only during episodes of acute illness. It may be that cardiomyopathy occurs only after prolonged exposure to high levels of malonate.

It is also interesting to speculate that the developmental delay associated with MCD deficiency is due to the inhibition of peroxisomal beta-oxidation. The endogenous synthesis of certain polyunsaturated fatty acids (PUFA) known to be critical for normal brain development requires peroxisomal beta-oxidation (Anderson et al. 1990; Moore et al. 1995). The pattern of MCD activity in the developing brain would support the idea of an important role for this protein (Dickson et al. 1994). The inhibition of endogenous PUFA synthesis may also mediate the reported effect of mild MCD deficiency as a risk factor for hyperlipidemia (Halliday et al. 1988; Nydahl et al. 1994). This effect will be of particular interest, since it may lead to the development of novel therapeutic approaches to MCD deficiency.

Acknowledgments

We acknowledge the resources provided by HGMP, particularly in the supply of IMAGE clones and de Jong RPCI1 gridded PAC library-screening pools. This work was partly funded by the Wellcome Trust.

Electronic-Database Information

Accession numbers and URLs for data in this article are as follows:

ClustalW interactive analysis program, http://www2.ebi.ac.uk/services.html (for sequence-alignment analysis)

dbEST, http://www.ncbi.nlm.nih.gov/dbEST/index.html (for gMCDp sequence data)

ESTblast program, http://gcg.hgmp.mrc.ac.uk/cgi-bin/Est_blast/Est_blast/ESTblast.pl (for sequence-data analysis)

GenBank, http://www.ncbi.nlm.nih.gov/Web/Search (for ESTs [AF097832, P12617, and Z46242])

Online Mendelian Inheritance in Man (OMIM), http://www.ncbi.nlm.nih.gov/Omim/ (for MCD deficiency [MIM 248360])

TransTerm database, http://biochem.otago.ac.nz:800/Transterm/ (for sequence data)

References

Abdel-Aleem S, St Louis J, Hendrickson SC, El-Shewy HM, El-Dawy K, Taylor DA, Lowe JE (1998) Regulation of carbohydrate and fatty acid utilization by L-carnitine during cardiac development and hypoxia. Mol Cell Biochem 180: 95–103

A'Bhaird NN, Ramsay RR (1992) Malonyl-CoA inhibition of peroxisomal carnitine octanoyltransferase. Biochem J 286: 637–640

Aeib H (1974) Catalase. In: Bergmeyer HU (ed) Methods of enzymatic analysis. Academic Press, New York, pp 673–684

Altschul SF, Gish W, Miller W, Myers EW, Lipman DJ (1990) Basic local alignment search tool. J Mol Biol 215:403–410

Anderson GJ, Connor WE, Corliss JD (1990) Docosahexaenoic acid is the preferred dietary n-3 fatty acid for the development of the brain and retina. Pediatr Res 27:89–97

Axton R, Hanson I, Danes S, Sellar G, van Heyningen V, Prosser J (1997) The incidence of PAX6 mutation in patients with simple aniridia: an evaluation of mutation detection in 12 cases. J Med Genet 34:279–286

Bergmeyer HU, Bernt E (1974) Lactate dehydrogenase: UV-assay with pyruvate and NADH. In: Bergmeyer HU (ed) Methods of enzymatic analysis. Academic Press, New York, pp 574–579

Brown GK, Scholem RD, Bankier A, Danks DM (1984) Malonyl coenzyme A decarboxylase deficiency. J Inherit Metab Dis 7:21–26

Claros MG, Vincens P (1996) Computational method to predict mitochondrially imported proteins and their targeting sequences. Eur J Biochem 241:779–786

Courchesne Smith C, Jang SH, Shi Q, Dewille J, Sasaki G, Kolattukudy PE (1992) Cytoplasmic accumulation of a normally mitochondrial malonyl-CoA decarboxylase by the use of an alternate transcription start site. Arch Biochem Biophys 298:576–586

Dickson AC, McEvoy JA, Koeppen AH (1994) The cellular localization of malonyl-coenzyme A decarboxylase in rat brain. Neurochem Res 19:1271–1276

Dyck JR, Barr AJ, Barr RL, Kolattukudy PE, Lopaschuk GD (1998) Characterization of cardiac malonyl-CoA decarboxylase and its putative role in regulating fatty acid oxidation. Am J Physiol 275:H2122–2129

Fox RM (1971) A simple incubation flask for 14CO2 collection. Anal Biochem 41:578–580

Geelen MJ, Bijleveld C, Velasco G, Wanders RJ, Guzman M (1997) Studies on the intracellular localization of acetyl-CoA carboxylase. Biochem Biophys Res Commun 233:253–257

Gould SJ, Keller GA, Schneider M, Howell SH, Garrard LJ, Goodman JM, Distel B, et al (1990) Peroxisomal protein import is conserved between yeast, plants, insects and mammals. EMBO J 9:85–90

Haan EA, Scholem RD, Croll HB, Brown GK (1986) Malonyl-CoA decarboxylase deficiency; clinical and biochemical findings in a second child with a more severe enzyme defect. Eur J Pediatr 144:567–570

Hall JL, Lopaschuk GD, Barr A, Bringas J, Pizzurro RD, Stanley WC (1996) Increased cardiac fatty acid uptake with dobutamine infusion in swine is accompanied by a decrease in malonyl CoA levels. Cardiovasc Res 32:879–885

Halliday JL, Brown GK, Danks DM (1988) Is mild deficiency of mitochondrial malonyl CoA decarboxylase a risk factor for hyperlipidemia? Biochem Med Metab Biol 39:279–283

Hsieh YJ, Kolattukudy PE (1994) Inhibition of erythromycin synthesis by disruption of malonyl-coenzyme A decarboxylase gene eryM in Saccharopolyspora erythraea. J Bacteriol 176:714–724

Jang SH, Cheesbrough TM, Kolattukudy PE (1989) Molecular-cloning, nucleotide-sequence, and tissue distribution of malonyl-CoA decarboxylase. J Biol Chem 264:3500–3505

Kim YS, Kolattukudy PE (1978*a*) Malonyl-CoA decarboxylase from the mammary gland of lactating rat: purification, properties and subcellular localization. Biochim Biophys Acta 531:187–196

Kim YS, Kolattukudy PE (1978*b*) Malonyl-CoA decarboxylase from the uropygial gland of waterfowl: purification, properties, immunological comparison, and role in regulating the synthesis of multimethyl-branched fatty acids. Arch Biochem Biophys 190:585–597

Kolattukudy PE, Rogers LM, Poulose AJ, Jang SH, Kim YS, Cheesbrough TM, Liggitt DH (1987) Developmental pattern of the expression of malonyl-CoA decarboxylase gene and the production of unique lipids in the goose uropygial glands. Arch Biochem Biophys 256:446–454

Krawinkel MB, Oldigs HD, Santer R, Lehnert W, Wendel U, Schaub J (1994) Association of malonyl-CoA decarboxylase deficiency and heterozygote state for hemoglobin-C disease. J Inherit Metab Dis 17:636–637

Lowry OH, Rosenbrough NJ, Farr AL, Randall RJ (1951) Protein measurement with the folin phenol reagent. J Biol Chem 193:265–275

MacPhee GB, Logan RW, Mitchell JS, Howells DW, Tsotsis E, Thorburn DR (1993) Malonyl coenzyme A decarboxylase deficiency. Arch Dis Child 69:433–436

Matalon R, Michaels K, Kaul R, Whitman V, Rodriguez-Novo J, Goodman S, Thorburn DR (1993) Malonic aciduria and cardiomyopathy. J Inherit Metab Dis 16:571–573

Moore SA, Hurt E, Yoder E, Sprecher H, Spector AA (1995) Docosahexaenoic acid synthesis in human skin fibroblasts involves peroxisomal retroconversion of tetracosahexaenoic acid. J Lipid Res 36:2433–2443

Nydahl MC, Gustafsson IB, Vessby B (1994) Lipid-lowering diets enriched with monounsaturated or polyunsaturated fatty acids but low in saturated fatty acids have similar effects on serum lipid concentrations in hyperlipidemic patients. Am J Clin Nutr 59:115–122

Rust S, Funke H, Assmann G (1993) Mutagenically separated PCR (MS-PCR): a highly specific one step procedure for easy mutation detection. Nucleic Acids Res 21:3623–3629

Saiki RK, Gelfand DH, Stoffel S, Scharf SJ, Higuchi R, Horn GT, Mullis KB, et al (1988) Primer-directed enzymatic amplification of DNA with a thermostable DNA polymerase. Science 239:487–491

Scholte HR (1969) The intracellular and intramitochondrial distribution of malonyl-CoA decarboxylase and propionyl-CoA carboxylase in rat liver. Biochim Biophys Acta 178: 137–144

Schuler GD, Boguski MS, Stewart EA, Stein LD, Gyapay G, Rice K, White RE, et al (1996) A gene map of the human genome. Science 274:540–546

Shepard D, Garland PB (1969) Citrate synthase from rat liver. Methods Enzymol 13:11–16

Shi J, Zhu H, Arvidson DN, Cregg JM, Woldegiorgis G (1998) Deletion of the conserved first 18 N-terminal amino acid residues in rat liver carnitine palmitoyltransferase I abolishes malonyl-CoA sensitivity and binding. Biochemistry 37: 11033–11038

Singh H, Poulos A (1988) Distinct long chain and very long chain fatty acyl-CoA synthetases in rat liver peroxisomes and microsomes. Arch Biochem Biophys 266:486–495

Sottocasa GL, Kuylenstierna B, Ernste L, Bergstrand A (1967) An electron-transport system associated with the outer membrane of liver mitochondria. J Cell Biol 32:415–438

Udenfriend S, Stein S, Böhlen P, Dairman W, Leimgruber W, Weigele M (1972) Fluorescamine: a reagent for assay of amino acids, peptides, proteins and primary amines in the picomole range. Science 178:871–872

Yano S, Sweetman L, Thorburn DR, Mofidi S, Williams JC (1997) A new case of malonyl coenzyme A decarboxylase deficiency presenting with cardiomyopathy. Eur J Pediatr 156:382–383

Zhang S, Kim KH (1996) Acetyl-CoA carboxylase is essential for nutrient-induced insulin secretion. Biochem Biophys Res Commun 229:701–705